PNAS RESEARCH ARTICLE | EVOLUTION

# Cranial modularity drives phenotypic diversification and adaptive radiation of Antarctic icefishes

Mayara P. Neves[a,b,1], HoWan Chan[a], Elizabeth C. M. Santos[c,d], and Kory M. Evans[a]

Edited by Scott Edwards, Harvard University, Cambridge, MA; received February 17, 2025; accepted August 13, 2025

**Modularity among traits is thought to drive morphological evolution and diversification, with more modular species often showing greater morphological disparity and faster evolutionary rates. However, recent studies suggest this pattern is not universal, as higher integration can sometimes be linked to faster rates of evolution. In adaptive radiation, modularity likely facilitates morphological divergence, but its specific role in trait diversification within these events remains uncertain. Antarctic icefishes (Perciformes: Notothenioidei) have undergone adaptive radiation in the frigid Southern Ocean, yet the role of modularity in their craniofacial evolution remains poorly understood. Emerging from a common ancestor 22 Mya, these fishes developed unique morpho-physiological adaptations, such as antifreeze glycoproteins, that contributed to their evolutionary success, but the contribution of cranial modularity to their diversification is still unexplored. Here, we analyze skull shape across 172 perciform species using micro-CT scanning and geometric morphometrics to investigate the tempo and mode of skull evolution in 80 notothenioids versus 92 perciform relatives. Notothenioids exhibit considerable cranial shape diversity, with skull shapes ranging from short to long faces. Fast rates of skull shape evolution occurred in smaller subclades following the emergence of cranial elongation, a derived trait within notothenioids. They also exhibit elevated evolutionary modularity relative to their perciform relatives, with reduced covariation among skeletal elements over time, likely corresponding with Miocene cooling events and the formation of the Antarctic Circumpolar Current. We propose that greater phenotypic modularity in notothenioid skulls represents a pivotal innovation, facilitating their evolutionary response to new ecological opportunities in the Antarctic.**

Antarctica | climatic change | skull | morphological evolution | fish

## Significance

Antarctic notothenioid fishes are a prime example of adaptive radiation in one of Earth's harshest environments. This study examines how changes in skull shape, driven by cranial modularity, have influenced their evolutionary success. By comparing skull evolution in notothenioids to related species, we show that increased modularity in their skulls has likely allowed for faster and more diverse adaptations to new ecological challenges, especially during major climatic shifts like the Miocene cooling. This study sheds light on the important role of modularity in driving the evolution of species in extreme environments, offering insights into the broader processes of adaptive radiation.

Modularity is a ubiquitous feature of organismal architecture. Traits are organized into modules where the degree of covariation within a given module is greater than the degree of covariation between modules (1). These modules form the building blocks of organismal structure and evolution (2, 3). This organization and compartmentalization of different sets of traits allows them to vary and evolve quasi-independently, potentially circumventing constraints associated with selection affecting other traits (4). These modules can then exhibit differential responses to selective pressures, resulting in functional specialization within an organism (5). Over time, the quasi-independence of modules can result in mosaic patterns of evolution where different modules or traits exhibit different tempos and modes of evolution (6, 7). Thus, modularity is thought to function as a core process of morphological evolution. However, despite its importance, the specific effect of modularity on patterns of morphological evolution is less clear. Some studies have found that strong modularity results in rapid rates of trait evolution while other studies have found accelerated rates of evolution under reduced modularity (higher integration) (8–11). Other studies still have found highly conserved patterns of modularity despite immense morphological diversity and rapid rates of morphological evolution (12, 13). As such, the question of how modularity is related to morphological diversification remains unanswered. Understanding this relationship becomes particularly important in systems characterized by rapid bursts of morphological evolution, such as adaptive radiations, where selection pressures are intense and trait innovation is often accelerated.

Adaptive radiations represent unique episodes of rapid speciation coupled with ecomorphological diversification and have produced a stunning diversity of forms ranging from the bills and jaws of Hawaiian Honey Creepers and African Rift Lake Cichlids to the diverse body shapes of Anolis lizards, which have adapted to distinct ecological niches such as tree trunks, grass, and canopy perches in the Caribbean (14–16). These adaptive radiations give us a unique glimpse into the effects of strong ecologically driven selection on phenotypic evolution. However, while the external ecological drivers of adaptive

Author affiliations: [a]Department of Biosciences, Rice University, Houston, TX 77005; [b]Department of Zoology, Universidade Federal do Paraná, Curitiba, PR 81530-000, Brazil; [c]Department of Biology, University of Oklahoma, Norman, OK 73019; and [d]Department of Evolution, Ecology and Organismal Biology, The Ohio State University, Columbus, OH 43212

Author contributions: M.P.N. and K.M.E. designed research; M.P.N., H.C., E.C.M.S., and K.M.E. performed research; K.M.E. contributed new reagents/analytic tools; M.P.N., H.C., E.C.M.S., and K.M.E. analyzed data; and M.P.N. and K.M.E. wrote the paper.

The authors declare no competing interest.

This article is a PNAS Direct Submission.



[1]To whom correspondence may be addressed. Email: mayara.neves@ufpr.br.

This article contains supporting information online at https://www.pnas.org/lookup/suppl/doi:10.1073/pnas.2503283122/-/DCSupplemental.

Published September 29, 2025.

divergence are often well-understood, much less is known about the role that modularity plays in the rapid evolution of these specialized phenotypes. This represents a large gap in our understanding of adaptive evolution because modularity can strongly influence the evolvability of different traits allowing some traits to become more evolutionarily labile while constraining the range of variation in others (3, 17, 18). Within adaptive radiation, differences in evolvability can be important because they may determine which traits will be more likely to be recruited to respond to different environmental stimuli. Some studies have found distinct patterns of modularity across different ecomorphs within an adaptive radiation (19). In contrast, other studies have found that while overall modularity patterns are conserved during a radiation, the degree of covariation among traits within modules can vary substantially between species. This can allow for a partial decoupling of some traits with a modular network while others become more tightly integrated (13). In addition to facilitating adaptive ecomorphological diversification, some evidence suggests that patterns of trait covariation can change in response to environmental fluctuations which can add an additional layer of complexity. If environmental shifts create novel ecological opportunities, it may also restructure patterns of modularity and allow organisms to explore different trait combinations as they adapt to changing environmental conditions (20). Under these circumstances, it becomes critically important to understand how traits covary and coevolve during these rapid periods of evolutionary divergence.

Antarctic icefishes (Notothenioidei, Perciformes) represent an exciting system to study the role of modularity during adaptive radiation and adaptation to shifting environmental conditions (21, 22). Notothenioids are a member of the hyperdiverse Perciformes clade and now represent the most diverse, abundant, vertebrate group in the Southern Ocean, with over 155 fish species belonging to 7 families (23–25). In addition to dominating the vertebrate fauna in Antarctica, there are three non-Antarctic families, which include the thornfish family Bovichtidae and two monotypic families, Pseudaphritidae and Eleginopsidae, that are distributed around the coast of southern America, Australia, New Zealand, and Sub Antarctic Islands (26). The cryonotothenioids or the "Antarctic clade" (27) are restricted to Antarctica, where they experience near freezing conditions and exhibit striking physiological and biochemical adaptations of these extreme conditions such as antifreeze glycoproteins—AFGPs (28), loss of hemoglobin and myoglobin expression resulting in transparent blood (29, 30), and metabolic adaptations suitable for energy tuning in frigid extremes. Moreover, notothenioids show benthic-pelagic transitions, and pelagic members have unique strategies for buoyancy control, such as reducing skeletal ossification and extensive lipid deposits, compensating for the lack of swim bladders (31, 32). In addition to their physiological adaptations, notothenioid fishes also exhibit broad craniofacial diversity that has been shown to strongly correlate with foraging habitat ranging from benthic predators which feed on invertebrates to secondarily evolved pelagic predators which feed on highly mobile nekton in the water column (28, 33–36).

These traits have collectively enabled notothenioids to thrive in the harsh Antarctic marine environment where other nearshore fish lineages have gone extinct, illustrating that their adaptive radiation is not limited to a single trait (35). In a previous study of head shape modularity within the icefishes, a strong pattern of integration between different regions of the head was reported where icefishes were found to exhibit stronger patterns of trait covariation than other nonicefish notothenioids. It was hypothesized that this strong integration allowed for rapid and coordinated trait divergence during adaptive diversification (33). However, since the previous study focused solely on the external morphology of the head (i.e., overall head shape), it remains unclear whether modularity within the skull itself plays an even greater role in shaping this diversification. By exploring the internal organization of the skull, modularity, and its potential to facilitate independent evolutionary changes across skull regions, we aim to uncover whether these internal patterns of organization underpin the extraordinary phenotypic diversity observed in notothenioids. Therefore, our study provides a perspective on how modularity influences the tempo and mode of cranial evolution.

Here, we employ a comprehensive, high-resolution geometric morphometric analysis across notothenioids and other perciform fishes, to study the role of modularity and environmental variation in the adaptive radiation of notothenioid fishes. We combine three-dimensional geometric morphometrics with a cutting-edge phylogenetic comparative method toolkit to analyze the tempo and mode of skull shape evolution in 80 notothenioid species and 92 outgroup perciform species. We explore whether the exceptional skull shape diversity of notothenioids relative to their perciform relatives stems from differences in i) evolutionary rates, and ii) the patterns of cranial integration and modularity. We hypothesize that notothenioids underwent a shift in their rates of skull shape evolution corresponding to their adaptive radiation in the Southern Ocean. Additionally, we hypothesize that notothenioids will exhibit higher levels of cranial modularity compared to their perciform relatives, allowing evolution of new adaptations for living in an extreme cold environment.

## Results

**Skull Shape Diversification in Notothenioidei and Other Perciformes.** Notothenioids exhibit considerable skull shape diversity, with most variation occurring along the first principal component (PC1), which is associated with skull length (Fig. 1 and *SI Appendix*, Fig. S1). This variation reflects an axis of broad cranial disparity, with skull shapes ranging from rounded and foreshortened to elongated. In our phylomorphospace analysis, notothenioids occupy both extremes along the PC1 axis relative to their perciform relatives, with the Yellowbelly rockcod (*Notothenia neglecta*) showing the lowest score along PC1 and Mawson's dragonfish (*Cygnodraco mawsoni*) the highest. In contrast, most perciform species tend to exhibit relatively short skulls, with only a few displaying elongated forms (e.g., *Aulorhynchus flavidus*, *Ambiserrula jugosa*, *Platycephalus indicus*, *Rogadius pristiger*, and *Scalicus amiscus*; *SI Appendix*, Fig. S1). Skull shape variation is further associated with skull depth along the second principal component (PC2) axis. Here, the nonnotothenioid Perciformes predominantly occupy the lower left quadrant of the morphospace (negative scores on both PC1 and PC2), with species like the Barred soapfish (*Diploprion bifasciatum*) and the Barred hamlet (*Hypoplectrus puella*) exhibiting the lowest scores with short deep and laterally compressed skulls. In contrast, higher positive scores on the PC2 axis are associated with more dorsoventrally compressed species and with the eye sockets positioned more dorsally, such as the notothenioids Congolli (*Pseudaphritis urvillii*) and Brainbeard plunderfish (*Pogonophryne cerebropogon*). Overall, phylogenetic signal analysis reveals a significant but weak phylogenetic structure in skull shape across the entire clade (Blomberg's K = 0.154; $P$ = 0.001), which may be driven not only by convergent evolution in both notothenioids and perciforms with elongated skulls but also by the high morphological diversity within notothenioids. Possibly due to the same reason, there was no significant difference in

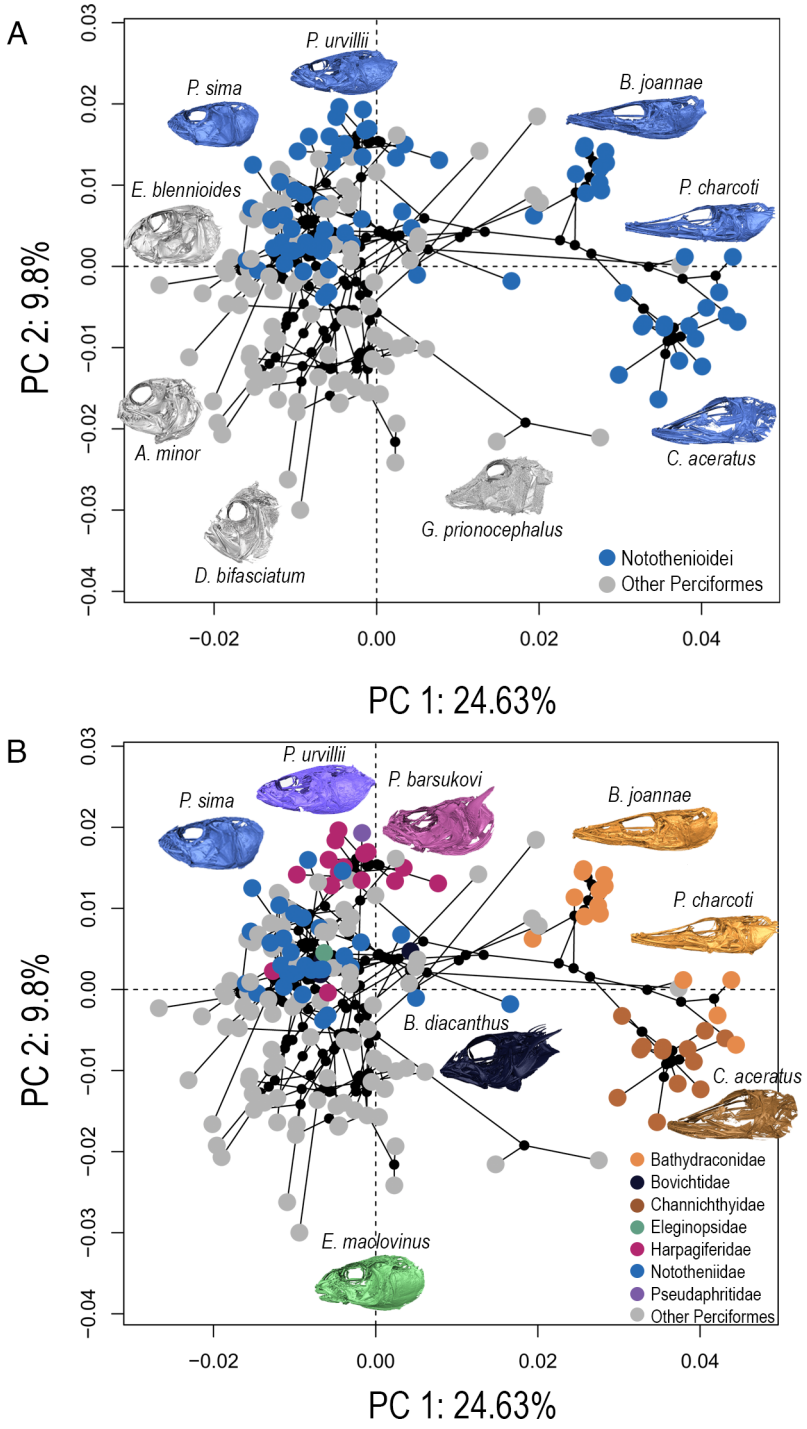


**Fig. 1.** Phylomorphospace analysis showing the skull shape diversity and evolution across 80 notothenioids and 92 other perciform species (*A*), and according to the notothenioid families (*B*). *Insets* illustrate representative skull shapes for each group or family.

skull shape disparity between notothenioids and other perciforms (Procrustes variances: 0.001 for both groups, $P = 0.524$). These results suggest that perciforms in general are very diverse, but notothenioids contributed to this diversity by colonizing new areas of morphospace associated with skull elongation. Interestingly, we did not find a significant relationship between skull shape and any of the ecological predictors using our phylogenetic generalized least squares analysis (*SI Appendix*, Tables S1–S3).

**Tempo and Mode of Skull Shape Evolution.** Out of the seven models of trait evolution that we evaluated, we found the strongest support for a variable rate Brownian motion model of skull shape (*SI Appendix*, Fig. S5 and Table S9). Notothenioids display notably high rates of skull shape evolution at different taxonomic levels (Fig. 2). At the family level, this is especially apparent in the lineages of Harpagiferidae, Bathydraconidae, and Channichthyidae, where distinct shifts toward more elongated skull shapes occur independently across each clade (Fig. 1). Our variable rates analysis recovers a shift in the rate of skull shape evolution within a small subclade of the Notohinidae at the onset of the Miocene (~23 Ma) (37, 38) (Fig. 2*A*). We observe the most rapid rate shift within notothenioids at approximately 15 Ma which roughly aligns with the Miocene climatic optimum and a period of global climatic variability and several subsequent rate

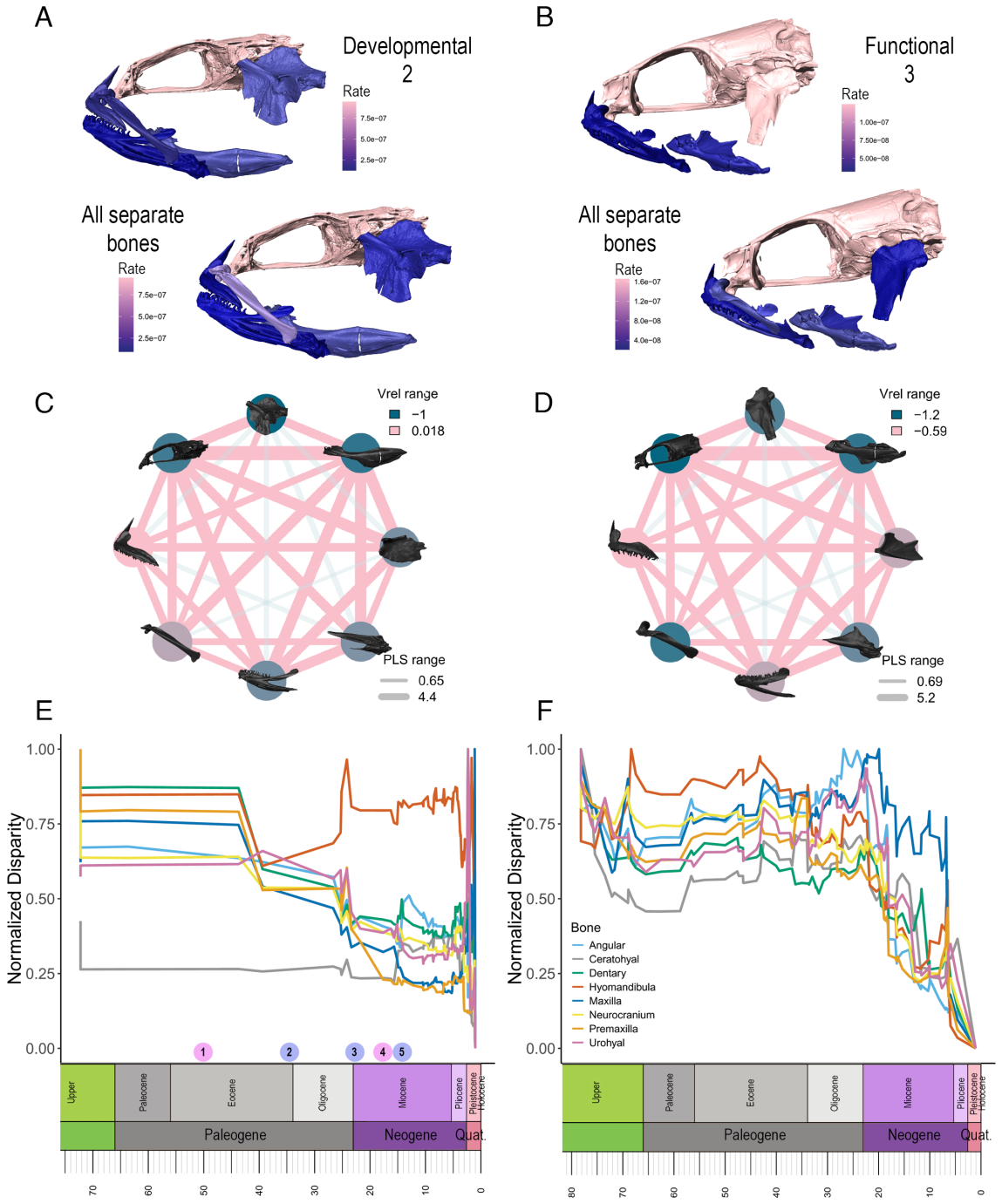


**Fig. 2.** Tempo of skull shape evolution in Perciformes, including notothenioids. Rate shifts of skull shape evolution estimated from BayesTraits mapped onto the time-calibrated phylogeny from Rabosky et al. (37) under the best-supported model of trait evolution (Brownian motion). Representative CT scans of notothenioid skulls are shown for branches of interest.

shifts in across the most of the notothenioid families throughout the Miocene and into the Pliocene.

Among the other Perciformes, the fastest evolutionary rates are observed in the suborder Cottoidei (37), a clade characterized by a broad range of habitats, ecological specializations, and adaptations to extreme environments, as exemplified by the families Abyssocottidae, Agonidae, Psychrolutidae, and Zoarcidae (38, 39). Comparisons of mean evolutionary rates between notothenioids and their relatives revealed significantly lower rates of skull shape evolution among notothenioids compared to other perciforms (rate ratio = 6.19; $P < 0.001$), defying our expectations. These findings suggest that other Perciformes, such as Cottoidei, exhibited higher overall rates of skull shape diversification compared to notothenioids, which displayed more variable rates of skull shape evolution within smaller subclades after evolving cranial elongation.

**Evolutionary Modularity and Integration.** We observed a higher degree of modularity within the skulls of notothenioids relative to other perciforms. Specifically, we found that the skulls of other perciforms were significantly more integrated than those of notothenioids (PLS effect sizes: other Perciformes = 2.88, notothenioids = 0.59, $P = 0.043$). For notothenioids, there was strong model support for the Developmental 2 hypothesis—a highly modular model consisting of upper jaws (premaxilla and maxilla), lower jaws (dentary and angular), neurocranium,

hyoid apparatus, and hyomandibula—followed by Functional 3, constituted by three modules—oral jaws, neurocranium and hyomandibula and hyoid apparatus (Table 1 and *SI Appendix*, Table S4). In contrast, for other Perciformes, the Functional 3 hypothesis had the strongest support, followed by Functional 4 and Developmental 2 (Table 1 and *SI Appendix*, Table S5). Additionally, in notothenioids, the highest evolutionary rates were consistently found in shape partitions that included the neurocranium and maxilla (Fig. 3*A* and *SI Appendix*, Table S6). Similarly, for other Perciformes, the highest evolutionary rates were observed for the neurocranium, whereas the slowest rates were found in modules containing the oral jaw bones, hyomandibula, ceratohyal, and urohyal (Fig. 3*B* and *SI Appendix*, Table S6).

The network analysis of cranial modularity reveals distinct patterns between notothenioids and other perciforms. In notothenioids (Fig. 3*C*), the connections between cranial modules are weaker, as indicated by thinner lines, and the observed Vrel range (relative eigenvalue index) is smaller, spanning from −1 to 0.018. Additionally, the PLS range (integration effect size) is primarily at the lower end, ranging from 0.65 to 4.4, which reflects lower levels of integration between cranial modules. In contrast, other Perciformes (Fig. 3*D*) show more densely connected cranial modules, represented by thicker lines, suggesting higher integration. The PLS range is also wider, from 0.69 to 5.2, reflecting stronger cranial integration.

The disparity-through-time analysis of overall skull shape diversity reveals contrasting evolutionary patterns between notothenioids (Fig. 3*E*) and other perciforms (Fig. 3*F*), indicating a decoupled pattern across partitions within notothenioids. Notothenioids initially exhibit high levels of normalized disparity during the Eocene, followed by a sharp decline around the late Eocene and Oligocene during the onset of Antarctic glaciation. During Mi1 Glaciation (first Miocene glaciation) at the beginning of the Miocene (23 Ma), there was an increase in disparity and a decoupled pattern across partitions, especially for hyomandibula, followed by a stabilization across the onset of Antarctic warming and the Middle Miocene climate transition. This pattern suggests early partitioning of skull shapes among clades likely driven by environmental changes during this dynamic period in the Southern Ocean. In contrast, other Perciformes show a more gradual and sustained decline in disparity, with multiple peaks with a similar tendency among cranial bones, with an increase in disparity in the Miocene, followed by a decline and stabilization at lower levels. This indicates that other Perciformes maintained more consistent rates of morphological evolution, perhaps reflecting their broader ecological diversity and adaptability across different habitats.

## Discussion

**Modularity Drives Mosaic Evolution of the Notothenioid Skull.** Adaptive radiations are episodes of rapid lineage diversification along ecomorphological lines (40). During these radiations, modularity likely plays a key role in structuring patterns of trait variation and diversification. Here, we examined the notothenioid radiation, which is thought to have been driven in part by the thermal isolation of Antarctica and has produced a broad diversity of ecomorphologies in the cranial region that corresponds to diet and foraging habitat (34). We find that notothenioids are on average more modular than their other perciform relatives and have further partitioned their skulls to include an additional module in the maxilla, which is a functionally relevant bone that influences suction-feeding kinematics (41). This increase in modularity may explain this clade's ability to take advantage of new ecological opportunities in a changing Antarctic ecosystem.

Modularity at evolutionary timescales has frequently been shown to result in mosaic patterns of trait evolution (6, 7, 42). Here, we find strong support for mosaic evolution across the skull of notothenioid and perciform fishes where in both groups the neurocranium exhibits significantly faster rates of shape evolution than any of the other modules. The neurocranium is a large, functionally complex region of the skull that houses the sensory capsules and provides numerous sites for muscle attachments. Neurocranium shape also has been shown to correlate with various aspects of ecomorphology including diet and behavior (43, 44). As notothenioid fishes are known to have adaptively radiated along habitat and trophic lines, it is possible that aspects of neurocranium shape evolution correspond with transitions to different habitats and diets across the radiation, though we did not find this in our analyses. While both perciforms and notothenioid fishes exhibit rapid rates of shape evolution in the neurocranium, differences in patterns of mosaic evolution are most evident in the oral jaws. In perciform fishes, the oral jaws constitute a single module that evolves slowly. However, notothenioid fishes have partitioned their oral jaws into two separate modules with the upper and lower jaws constituting separate modules. In notothenioid fishes the maxilla exhibits elevated rates of shape evolution relative to the surrounding bones of the oral jaws. The maxilla plays an important role in jaw protrusion in many suction-feeding teleost fishes (41, 45–47). This bone is highly mobile during jaw protrusion and the degree of rotation has been shown to predict the trophic ecology of several fish clades (47–49). Shape changes in the maxilla of notothenioid fishes may potentially reflect the diversity of trophic ecologies present in notothenioid fishes, ranging from benthic invertivores with short, strong jaws to fishes that feed on more mobile preying

**Table 1. Results of the evolutionary modularity tests using the CR for notothenioids and other perciforms**

| | | Notothenioids | | | Other perciforms | | |
|---|---|---|---|---|---|---|---|
| | Number of modules | CR | *P*-value | Effect size | CR | *P*-value | Effect size |
| Total integration | 1 | NA | NA | 0 | NA | NA | 0 |
| Functional 1 | 2 | 0.854 | 0.004 | −2.840 | 0.764 | 0.001 | −6.003 |
| Functional 2 | 2 | 0.789 | 0.001 | −4.422 | 0.820 | 0.001 | −4.593 |
| Functional 3 | 3 | 0.620 | 0.001 | **−5.179** | 0.763 | 0.001 | **−6.742** |
| Functional 4 | 4 | 0.660 | 0.001 | −4.653 | 0.666 | 0.001 | **−6.482** |
| Developmental 1 | 3 | 0.686 | 0.001 | −5.165 | 0.767 | 0.001 | −6.380 |
| Developmental 2 | 4 | 0.658 | 0.001 | **−6.069** | 0.693 | 0.001 | **−6.427** |
| All separate | 8 | 0.587 | 0.001 | −8.902 | 0.560 | 0.001 | −7.036 |

Bold fonts denote hypotheses that were found to be statistically equivalent based on pairwise comparisons of effect size.

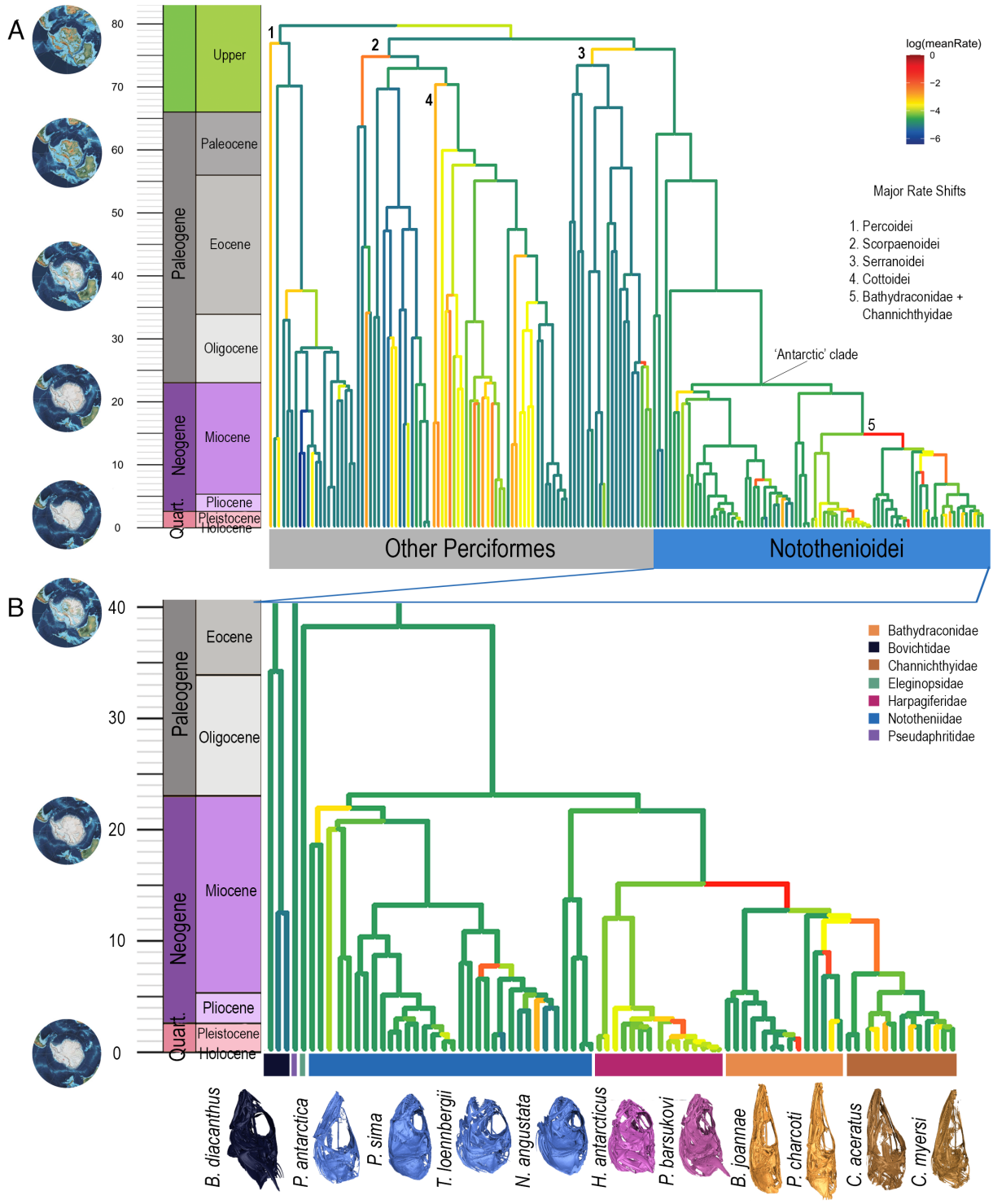


**Fig. 3.** Mode of skull shape evolution in notothenioid species and their relative perciforms. Evolutionary Brownian rate estimates for the best-fitting modularity hypothesis and for each separate cranial bone for notothenioids (*A*) and other perciforms (*B*). Network plots representing bone integration in notothenioids (*C*) and other perciforms (*D*). Nodes indicate within-bone integration, calculated using the relative eigenvalue index (Vrel), and lines represent between-bone integration, calculated using the rPLS value. Line thickness corresponds to higher integration values. The pink line indicates significant between-bone integration. Node colors reflect the magnitude of integration within each bone. Disparity though time analyses of each partition (bone) corrected by maximum rate value within each module for comparability showing shifts in the rate of skull shape evolution in notothenioids (*E*) and other perciforms (*F*). Major global paleoclimatic events since the Paleocene are highlighted with numerical circle: 1) Eocene Climatic Optimum, 2) Oligocene cooling Onset Antarctic glaciation, 3) Mi1 Glaciation, 4) Onset Antarctic warming, 5) Middle Miocene climate transition.

the water column, which require rapidly closing jaws (34). In a previous study of notothenioid head shape modularity, the authors reported broad patterns of integration across the head of channichthyid icefishes relative to other notothenioid species (33). In contrast, our study found elevated levels of modularity across a larger number of notothenioid species and includes an important outgroup comparison in Perciformes. Additionally, our study offers higher -resolution landmark coverage across the skull which has the potential to identify smaller and more localized patterns of trait variation and covariation.

Skull shape in vertebrates is shaped by a combination of ecological, functional, and developmental drivers that operate across diverse evolutionary contexts (50–54). Ecologically, the demands of feeding, sensory adaptation, and habitat utilization play pivotal roles in shaping skull morphology, with dietary specialization often dictating the mechanical properties and configurations of cranial structures, such as robust jaws in predators versus lightweight, streamlined skulls in filter feeders (55). Functionally, trade-offs between feeding efficiency, structural integrity, and sensory capabilities further influence cranial evolution, while developmental processes, including the organization of cranial modules and growth constraints, mediate evolutionary changes by enabling certain regions of the skull to evolve independently while maintaining overall functionality (56). In notothenioid fishes, these general drivers have been compounded by the extreme Antarctic environment, where thermal isolation and ecological opportunities have promoted unique patterns of skull evolution. The interplay between suction feeding and biting mechanics has likely been a critical functional driver, with distinct feeding strategies requiring specialized configurations of cranial bones (48, 57). For example, the decoupling of the maxilla in notothenioids may reflect adaptations for enhanced jaw protrusion, facilitating prey capture (i.e., zooplankton, invertebrates, and fish) in diverse trophic niches (58–60). Additionally, paleoclimatic events, such as the Miocene glaciation, may have created new ecological opportunities and selective pressures on cranial morphology, accelerating diversification. Together, these factors underscore how broad vertebrate trends intersect with the unique evolutionary history of notothenioids to produce their remarkable cranial diversity.

**Climatic Fluctuations Drive the Decoupling of the Notothenioid Skull.** Modularity has been predicted to increase the evolvability of complex trait systems by reducing the constraints associated with conditioning on other traits and by allowing modules to respond semiautonomously to different selective pressures (3, 61, 62). There is also additional evidence that the magnitude of modularity itself can change with fluctuations in environmental conditions where traits have been shown to exhibit more modularity in the face of more climatic variability (20). In our disparity through time (DTT) analysis of skull shape in notothenioids, we observe a decoupling in the accumulation of morphological disparity in the hyomandibula and premaxilla at the onset of the Miocene. Importantly, the onset of the Miocene epoch coincides with the Mi1 Glaciation of Antarctica which would have opened additional niches as less cold-tolerant fishes were driven to extinction (63, 64). Interestingly, we see no such pattern of decoupling in perciform fishes across the same timescale, suggesting that the more modular configuration of the notothenioid skull allowed the different regions of the skull to evolve semi-independently and capitalize on shifting environmental conditions.

**Antarctic Cycles of Glaciation as a Driver of Notothenioid Skull Shape Evolution.** Environmental factors played a crucial role in shaping the evolutionary trajectory of life on Earth (65, 66). Climatic shifts, such as the Miocene cooling events and the formation of the Antarctic Circumpolar Current, led to a dramatic cooling of the Southern Ocean, which likely created new ecological pressures that influenced the diversification of notothenioids (21). The adaptive significance of cranial elongation in notothenioids can be understood in the context of these environmental changes. Cranial elongation, a key morphological feature in many Antarctic species, appears to be a response to specialized feeding strategies and habitat use in the cold, nutrient-rich waters of the region. This elongation is closely linked to the ecological niches these fishes occupy, such as deep-water or benthic environments, where a streamlined skull shape enhances feeding efficiency and maneuverability, as well as contributes to the reduction of bone density (21). Furthermore, the modularity in craniofacial traits allowed for rapid adaptive responses to these changing environmental conditions, enabling notothenioids to exploit various niches in the Southern Ocean and contributing to their remarkable diversification. The interplay between these abiotic factors and cranial adaptations highlights how environmental pressures can drive morphological evolution through the modulation of key traits.

Herein, Antarctic notothenioids provide an ideal system for exploring how modularity can drive evolutionary radiation. While previous studies have emphasized their physiological innovations, such as antifreeze glycoproteins, our findings highlight the critical role of craniofacial modularity in enabling the morphological flexibility necessary to exploit diverse ecological niches. Therefore, this study provides valuable insights into the link between modularity and adaptive radiations, particularly in extreme environments like the Southern Ocean. Our findings suggest that modularity played a key role in coordinating changes across different traits, especially during the colonization of deep demersal habitats in the Southern Ocean by some notothenioid families. By highlighting the role of craniofacial modularity in the rapid diversification of notothenioids, this study advances our understanding of how trait decoupling can facilitate evolutionary innovation and ecological specialization. These findings open several avenues for future research, including investigating the genetic and developmental mechanisms underlying modularity and how they influence morphological evolution. Ultimately, this research has the potential to inform evolutionary studies across diverse taxa, shedding light on the fundamental processes that drive diversification and adaptation in response to environmental challenges, especially under climatic changes in the Anthropocene.

## Materials and Methods

**Morphological Sampling and Shape Analyses.** To investigate skull shape evolution in Notothenioidei, we quantified the skull shapes of 80 Notothenioidei species (representing approximately 51% of total clade diversity, with all seven families included) and 92 species from other Perciformes (encompassing 30 different families). This dataset includes a total of 172 species belonging to 37 families, covering 66% of the Perciformes families (*SI Appendix*, Fig. S1 and Table S7). We analyzed the three-dimensional skull morphology of each species through micro-computed tomography (μCT) scans (67). The specimens were scanned at both Rice University and the Natural History Museum of Los Angeles County (LACM) under the oVert and ScanAllFishes initiatives. Additionally, we obtained further scans from Morphosource (http://morphosource.org). These scans were processed in Amira v2.0.0 (Thermo Fisher Scientific, Waltham, MA) to isolate the skull by removing scales and other debris. The resulting skulls were converted into 3D meshes and saved as *.ply* files. We then digitized the mesh files with 145 three-dimensional landmarks (comprising both 55 fixed and 90 sliding semi-landmarks; *SI Appendix*, Fig. S2 and Table S8) using the Checkpoint software (Stratovan, Davis, CA). All landmarks were consistently placed on the left side of the skull.

The following eight bones were included in the analysis: neurocranium, premaxilla, maxilla, dentary, articular, hyomandibula, ceratohyal, and urohyal (*SI Appendix*, Fig. S2). Each of these bones were selected due to their functional relevance and evolutionary importance during the diversification of Notothenioidei and other Perciformes. The neurocranium forms the basic structure of the braincase, housing the brain and sensory organs. In ray-finned fishes, it consists of several bones, including the ethmoid, sphenotic, parasphenoid, supraoccipital, postorbital, and exoccipital, which together protect the brain and provide attachment points for muscles. The premaxilla, dentary, articular, and

maxilla are critical for prey capture and jaw protrusion while the hyomandibula, ceratohyal, and urohyal are involved buccal expansion and respiration (68).

After digitization, to account for rotation and translation inherent in the highly kinetic articulating components of the fish skull, we first aligned each dataset using Generalized Procrustes Analysis with the *gpagen* function in the *geomorph* package, version 4.0.8 (69) in R, version 4.4.1 (70). Next, a local superimposition was performed to standardize the positioning of the various skull elements (71, 72). To analyze the shape evolution of individual bones, we subdivided our comprehensive skull shape dataset into smaller datasets for each bone, with the raw coordinates for each bone individually superimposed. Following the local superimposition, using the *findmeanspecies* function, we determined the mean species shape for each group (Notothenioidei and Other Perciformes). After performing the local superimposition, we conducted a Principal Components (PCs) Analysis to explore the primary axes of skull shape variation. Additionally, we utilized the *plotRefToTarget* function in the *geomorph* package to illustrate the main axes of skull shape variation as ball-and-stick plots (*SI Appendix*, Fig. S3).

**Phylomorphospace and Morphological Disparity.** To visualize the major axes of shape variation and evolution of Notothenioidei, we employed a phylomorphospace approach using the first two PCs of shape variation (73), which accounted for 56% of the total shape variance, and the pruned, time-calibrated phylogeny (*SI Appendix*, Fig. S4) from Rabosky et al. (37). We pruned the phylogeny using the *drop.tip* function in the *ape* package version 5.0 (74) to only include the taxa present in our study. Additionally, we assessed the phylogenetic signal in our shape data using the multivariate implementation of Blomberg's K ($k_{mult}$) (75, 76) to test for phylogenetic structure within our skull shape dataset. To evaluate the morphological disparity in skull shape, we used the *morphol.disparity* function (77) in the *geomorph* package for comparisons between Notothenioidei and other Perciformes. This function calculates morphological disparity by estimating Procrustes variance for each group from the residuals of a linear model.

To assess changes in subclade morphological disparity for Notothenioidei and other Perciformes, we employed a DTT analysis under a Brownian motion model (78). This approach tracks shifts in relative subclade disparity over time across each node in the phylogeny. We compared the observed disparity to that generated by a null Brownian motion model, simulated over 1,000 iterations. To quantify the differences between the observed and expected disparities, we calculated a morphological disparity index (MDI), which reflects the deviation in relative within-clade disparities from what is predicted under a Brownian motion model. A negative MDI suggests that disparity is distributed among subclades, often interpreted as evidence of an adaptive radiation (79, 80). Conversely, a positive MDI indicates that disparity is concentrated within subclades. Since MDI estimates at various time points can be prone to a high false-positive rate, we employed the two-tailed rank envelope method of Murrell (81) to evaluate significance. This method provides both an overall *P*-value and a *P*-interval, as the ranking process often results in ties. For this two-tailed test, *P*-values below 0.025 are considered significant.

**Tempo and Mode of Skull Shape Evolution.** We tested seven models of trait evolution for perciform fishes that included a single rate Brownian motion model that assumed a single constant rate of evolution across the tree, an early burst model of trait evolution that models a rapid increase in the rate of trait evolution followed by a slowdown in the rate of trait evolution, a single peak Ornstein–Uhlenbeck (OU) model that models stationary variance around a single adaptive peak, a multipeak OU model based on habitat categories which are known to be a strong driver of adaptive divergence among notothenioids (82), a diet-based multipeak OU model, a multipeak OU model that subdivided the species by family, and finally, we tested a variable rate Brownian motion model of skull shape evolution (*SI Appendix*, Fig. S5 and Table S9). For habitat categorization, we assigned species to habitat categories based on previous studies and compilations (83–85) (*SI Appendix*, Table S7). Habitats were divided into six categories: coastal demersal, deep-sea demersal, deep-sea pelagic, shallow pelagic (including coastal and offshore habitats), freshwater, and a combined brackish, estuarine, and diadromous state. Shallow versus deep-sea divisions were based on where the species predominately occurs, instead of its maximum depth of record. The "demersal" category is general and includes fishes found on or near the benthos, as opposed to being predominately found within the water column ("pelagic"). These habitats represent a summary of the commonly hypothesized axes of ecomorphological diversification in fishes (39, 83, 86–92). While each habitat category certainly contains further possible ecological subdivisions, our binning strategy attempts to maximize phylogenetic replication to increase statistical power for downstream phylogenetic comparative methods. For diet, each species was assigned to one of five trophic guilds: carnivorous (generalists consuming fish, cephalopods, crustaceans, polychaetes, and other invertebrates), insectivorous (primarily feeding on aquatic or terrestrial insects), omnivorous (consuming similar amounts of animal and plant/macroalgae materials), piscivorous (primarily fish-eating), and zooplanktivorous (feeding on microprey such as krill and fish larvae). Diet classification was derived from a literature review and information from FishBase (93). Species for which dietary information was unavailable in both the literature, and FishBase were categorized as "unknown." Finally, we tested a variable rate Brownian motion model of skull shape evolution. All model-fitting analyses were performed using the *BayesTraitsV4* software (94). This Bayesian approach employs a reversible-jump Markov chain Monte Carlo method to estimate the likelihood of rate shifts in continuous trait data throughout a phylogeny. This technique can identify clade- and species-specific rate changes. Given the challenges associated with evolutionary model fitting for high-dimensional data (95), we reduced the dimensionality by using the first 27 PCs, which explained 95% of the total shape variance. Following Evans et al. (44) approach, the PCs were scaled by a factor of 1,000 to address computational issues in *BayesTraits* with very small numerical values. We used uniform, noninformative priors and ran four independent chains of 200 million generations each, discarding the initial 1 million generations as burn-in. Sampling occurred every 2 million generations after convergence, utilizing a stepping-stone sampler. Convergence was assessed by rerunning the analysis and visually inspecting the trace of the marginal likelihoods using *Tracer* v1.7.1 (96). Model comparison was done by calculating Bayes factors from the marginal likelihoods of the models. The output from BayesTraits was analyzed using utility functions from the packages BTProcessR (v.0.0.1) (97) and BTRTools (0.0.0.9) (98). The variable rates model had the strongest support out of the six models, so we used the results of the variable-rate analyses produced a collection of phylogenies in which each branch was scaled according to its Brownian motion rate of evolution. To complement the variable rates analyses, we also measured the rate of shape evolution between Notothenioidei and other Perciformes, using the *compare.evol.rates* function in the *geomorph* package (69, 77). To determine significance, we employed a phylogenetic simulation approach, as detailed by Adams and Collyer (95).

In addition to evolutionary model fitting, we also tested the relationship between skull shape and each of our ecological categorizations using a phylogenetic generalized least squares analysis using the *procD.pgls* function in *geomorph* (75, 77).

**Evolutionary Modularity and Integration.** To investigate patterns of evolutionary modularity between Notothenioidei and other Perciformes species, we formulated seven a priori hypotheses of modularity based on various functional, and developmental, interactions from existing literature (41, 42, 99, 100), as well as an eight-module hypothesis focused on individual bones as a null model (*SI Appendix*, Fig. S6 and Table S10). We assessed modularity using the *phylo.modularity* function from the *geomorph* package, which employs the covariance ratio (CR) method. This method evaluates the relative strength of covariation between modules compared to the covariation within modules (101). A CR value less than 1 suggests a more modular configuration, whereas a CR value greater than 1 indicates reduced modularity. Subsequently, under the most supported hypothesis, we compared the effect sizes (indicating the strength of the modular signal) for Notothenioidei and other Perciformes using the *compare.CR* function in *geomorph*. The model with the lowest effect size was considered the best supported. To illustrate the outcomes of the modularity analyses, we generated network plots that display the extent of integration between each module by evaluating the within-module integration of individual bones via the relative eigenvector index (Vrel) (102, 103) using the *integration.Vrel* function from the *geomorph* (77, 102, 103). This metric measures the degree of covariation within each bone considered as an independent module. To examine group-level differences in integration, we applied the *compare.Zrel* function from *geomorph* to assess the effect sizes of within-module integration across species (77, 102).

To evaluate evolutionary integration, we used the *phylo.integration* function in *geomorph* (104). This approach employs a two-block partial least-squares analysis to measure the extent of shape covariation between proposed modules while accounting for phylogenetic nonindependence. The analysis was conducted separately for

Notothenioidei and other Perciformes species. Then, we compared effect sizes between groups using *compare.PLS* in the *geomorph* (77). Finally, we employed the *compare.multi.evol.rates* function from the *geomorph* package to examine the rates of evolution for bone modules in Notothenioidei versus other Perciformes species. This approach determines the evolutionary rate parameters ($\sigma 2$) for multivariate traits based on specified modules. To assess significance, we compared the observed rates against a null rate matrix generated from 1,000 random permutations.

**Data, Materials, and Software Availability.** Dataset and R script data have been deposited in Dryad (https://doi.org/10.5061/dryad.vq83bk44j) (105).

**ACKNOWLEDGMENTS.** We are grateful to the following museums and personnel for loaning several fish species to scan: Academy of Natural Sciences of Drexel University (ANSP) (Dr. Mariangeles Arce H. and Dr. Mark P. Sabaj), California Academy of Sciences (CAS) (Dave Catania), Field Museum of Natural History (FMNH) (Dr. Caleb McMahan and Susan Mochel), Museum of Comparative Zoology, Harvard University (MCZ) (Andrew Williston), Yale Peabody Museum of Natural History (YPM) (M.Sc. Gregory Watkins-Colwell and Dr. Tom Near), Biodiversity Research and Teaching Collections, Texas A&M University (TCWC) (Kevin W. Conway and Heather L. Prestrige), and National Museum of Natural History, Smithsonian Institution (USNM) (Diane Pitassy and Abigail Reft). We thank the oVert and ScanAllFishes initiatives for available fish scans on Morphosource, Dr. William Ludt, and Dr. Todd Clardy (Natural History Museum of Los Angeles County – LACM) for scanning 20 notothenioids fishes for free. E.C.M. was supported by NSF DBI-1906574, and K.M.E. was supported by NSF DEB-2237278.

1. M. L. Zelditch, A. Goswami, What does modularity mean? *Evol. Dev.* **23**, 377–403 (2021).
2. G. P. Wagner, L. Altenberg, Perspective: Complex adaptations and the evolution of evolvability. *Evol.* **50**, 967–976 (1996).
3. G. P. Wagner, M. Pavlicev, J. M. Cheverud, The road to modularity. *Nat. Rev. Genet.* **8**, 921–931 (2007).
4. G. P. Wagner, J. Zhang, The pleiotropic structure of the genotype-phenotype map: The evolvability of complex organisms. *Nat. Rev. Genet.* **12**, 204–213 (2011).
5. M. Linde-Medina, J. C. Boughner, S. E. Santana, R. Diogo, Are more diverse parts of the mammalian skull more labile? *Ecol. Evol.* **6**, 2318–2324 (2016).
6. R. N. Felice, A. Goswami, Developmental origins of mosaic evolution in the avian cranium. *Proc. Natl. Acad. Sci. U.S.A.* **115**, 555–560 (2018).
7. O. Larouche, S. M. Gartner, M. W. Westneat, K. M. Evans, Mosaic evolution of the skull in labrid fishes involves differences in both tempo and mode of morphological change. *Syst. Biol.* **72**, 419–432 (2023).
8. T. J. Sanger, D. L. Mahler, A. Abzhanov, J. B. Losos, Roles for modularity and constraint in the evolution of cranial diversity among anolis lizards. *Evolution* **66**, 1525–1542 (2012).
9. O. Larouche, M. L. Zelditch, R. Cloutier, Modularity promotes morphological divergence in ray-finned fishes. *Sci. Rep.* **8**, 7278 (2018).
10. K. M. Evans *et al.*, Integration drives rapid phenotypic evolution in flatfishes. *Proc. Natl. Acad. Sci. U.S.A.* **118**, e2101330118 (2021), 10.1073/pnas.2101330118.
11. E. M. Troyer *et al.*, Evolutionary innovation accelerates morphological diversification in pufferfishes and their relatives. *Evolution* **78**, 1869–1882 (2024), 10.1093/evolut/qpae127.
12. A. Watanabe *et al.*, Ecomorphological diversification in squamates from conserved pattern of cranial integration. *Proc. Natl. Acad. Sci. U.S.A.* **116**, 14688–14697 (2019).
13. H. Chan, E. Colaco, C. H. Martin, K. M. Evans, Adaptive radiation despite conserved modularity patterns in San Salvador Island Cyprinodon pupfishes and their hybrids. *Evol. J. Linn. Soc.* **3**, kzae013 (2024).
14. J. J. Kolbe, L. J. Revell, B. Szekely, E. D. Brodie, J. B. Losos, Convergent evolution of phenotypic integration and its alignment with morphological diversification in Caribbean Anolis ecomorphs. *Evolution* **65**, 3608–3624 (2011).
15. M. D. McGee *et al.*, Replicated divergence in cichlid radiations mirrors a major vertebrate innovation. *Proc. R. Soc. B: Biol. Sci.* **283**, 20151413 (2016).
16. M. Tokita, W. Yano, H. F. James, A. Abzhanov, Cranial shape evolution in adaptive radiations of birds: Comparative morphometrics of Darwin's finches and Hawaiian honeycreepers. *Philos. Trans. R. Soc. Lond. B Biol. Sci.* **372**, 20150481 (2017).
17. A. Goswami, J. B. Smaers, C. Soligo, P. D. Polly, The macroevolutionary consequences of phenotypic integration: From development to deep time. *Philos. Trans. R. Soc. Lond. B Biol. Sci.* **369**, 20130254 (2014).
18. C. P. Klingenberg, Morphological integration and developmental modularity. *Annu. Rev. Ecol. Evol. Syst.* **39**, 115–132 (2008).
19. L. R. Monteiro, M. R. Nogueira, Adaptive radiations, ecological specialization, and the evolutionary integration of complex morphological structures. *Evolution* **64**, 724–744 (2010).
20. A. V. Badyaev, K. R. Foresman, R. L. Young, Evolution of morphological integration: Developmental accommodation of stress-induced variation. *Am. Nat.* **166**, 382–395 (2005).
21. J. M. Daane, H. William Detrich III, Adaptations and diversity of Antarctic fishes: A genomic perspective. *Annu. Rev. Anim. Biosci.* **29**, 25 (2025).
22. I. Bista *et al.*, Genomics of cold adaptations in the Antarctic notothenioid fish radiation. *Nat. Commun.* **14**, 3412 (2023).
23. J. T. Eastman, R. R. Eakin, Checklist of the species of notothenioid fishes. *Antarct. Sci.* **33**, 273–280 (2021).
24. E. Parker, A. Dornburg, C. D. Struthers, C. D. Jones, T. J. Near, Phylogenomic species delimitation dramatically reduces species diversity in an Antarctic adaptive radiation. *Syst. Biol.* **71**, 58–77 (2022).
25. R. Fricke, W. N. Eschmeyer, R. van der Laan, Eschmeyer's catalog of fishes: Genera, species, references (2024). http://researcharchive.calacademy.org/research/ichthyology/catalog/fishcatmain.asp.
26. C. Papetti *et al.*, Non-Antarctic notothenioids: Past phylogenetic history and contemporary phylogeographic implications in the face of environmental changes. *Mar. Genomics* **25**, 1–9 (2016).
27. T. J. Near *et al.*, Identification of the notothenioid sister lineage illuminates the biogeographic history of an Antarctic adaptive radiation. *BMC Evol. Biol.* **15**, 109 (2015).
28. J. T. Eastman, *Antarctic Fish Biology: Evolution in a Unique Environment* (Academic Press, 2013).
29. J. M. Daane *et al.*, Developmental constraint shaped genome evolution and erythrocyte loss in Antarctic fishes following paleoclimate change. *PLoS Genet.* **16**, e1009173 (2020).
30. T. Desvignes, I. Bista, K. Herrera, A. Landes, J. H. Postlethwait, Cold-driven hemoglobin evolution in Antarctic notothenioid fishes prior to hemoglobin gene loss in white-blooded icefishes. *Mol. Biol. Evol.* **40**, msad236 (2023).
31. J. T. Eastman, The buoyancy-based biotope axis of the evolutionary radiation of Antarctic cryonotothenioid fishes. *Polar Biol.* **43**, 1217–1231 (2020).
32. G. M. Castiglione, F. E. Hauser, A. Nynatten, B. S. W. Chang, Adaptation of Antarctic icefish vision to extreme environments. *Mol. Biol. Evol.* **40**, msad030 (2023).
33. Y. Hu *et al.*, Evolution in an extreme environment: Developmental biases and phenotypic integration in the adaptive radiation of Antarctic notothenioids. *BMC Evol. Biol.* **16**, 142 (2016).
34. E. Parker *et al.*, Periodic environmental disturbance drives repeated ecomorphological diversification in an adaptive radiation of Antarctic fishes. *Am. Nat.* **200**, E221–E236 (2022).
35. T. J. Near *et al.*, Ancient climate change, antifreeze, and the evolutionary diversification of Antarctic fishes. *Proc. Natl. Acad. Sci. U.S.A.* **109**, 3434–3439 (2012).
36. M. Mesa, J. T. Eastman, M. Vacchi, The role of notothenioid fish in the food web of the Ross Sea shelf waters: A review. *Polar Biol.* **27**, 321–338 (2004).
37. D. L. Rabosky *et al.*, An inverse latitudinal gradient in speciation rate for marine fishes. *Nature* **559**, 392–395 (2018).
38. M. D. Burns *et al.*, High-latitude ocean habitats are a crucible of fish body shape diversification. *Evol. Lett.* **8**, 669–679 (2024), 10.1093/evlett/qrae020.
39. T. J. Buser *et al.*, Freshwater habitats promote rapid rates of phenotypic evolution in sculpin fishes (Perciformes: Cottoidea). *Am. Nat.* **204**, 345–360 (2024), 10.1086/731784.
40. D. Schluter, *The Ecology of Adaptive Radiation* (OUP Oxford, 2000).
41. M. W. Westneat, Skull biomechanics and suction feeding in fishes. *Fish Physiol.* **23**, 29–75 (2005).
42. K. M. Evans, M. Vidal-García, V. A. Tagliacollo, S. J. Taylor, D. B. Fenolio, Bony patchwork: Mosaic patterns of evolution in the skull of electric fishes (Apteronotidae: Gymnotiformes). *Integr. Comp. Biol.* **59**, 420–431 (2019).
43. K. M. Evans, L. Y. Kim, B. A. Schubert, J. S. Albert, Ecomorphology of neotropical electric fishes: An integrative approach to testing the relationships between form, function, and trophic ecology. *Integr. Org. Biol.* **1**, obz015 (2019).
44. K. M. Evans, O. Larouche, J. J. L. West, S. M. Gartner, M. W. Westneat, Burrowing constrains patterns of skull shape evolution in wrasses. *Evol. Dev.* **25**, 73–84 (2023).
45. M. W. Westneat, Evolution of levers and linkages in the feeding mechanisms of fishes. *Integr. Comp. Biol.* **44**, 378–89 (2004).
46. P. Wainwright *et al.*, Suction feeding mechanics, performance, and diversity in fishes. *Integr. Comp. Biol.* **47**, 96–106 (2007).
47. M. Mihalitsis, P. C. Wainwright, Feeding kinematics of a surgeonfish reveal novel functions and relationships to reef substrata. *Commun. Biol.* **7**, 13 (2024).
48. D. C. Collar, P. C. Wainwright, M. E. Alfaro, L. J. Revell, R. S. Mehta, Biting disrupts integration to spur skull evolution in eels. *Nat. Commun.* **5**, 5505 (2014).
49. S. J. Longo, M. D. McGee, C. E. Oufiero, T. B. Waltzek, P. C. Wainwright, Body ram, not suction, is the primary axis of suction-feeding diversity in spiny-rayed fishes. *J. Exp. Biol.* **219**, 119–128 (2016).
50. F. O. Silva *et al.*, The ecological origins of snakes as revealed by skull evolution. *Nat. Commun.* **9**, 376 (2018).
51. K. E. Jones, L. Benitez, K. D. Angielczyk, S. E. Pierce, Adaptation and constraint in the evolution of the mammalian backbone. *BMC Evol. Biol.* **18**, 172 (2018).
52. R. N. Felice, J. A. Tobias, A. L. Pigot, A. Goswami, Dietary niche and the evolution of cranial morphology in birds. *Proc. R. Soc. B: Biol. Sci.* **286**, 20182677 (2019).
53. C. Bardua *et al.*, Size, microhabitat, and loss of larval feeding drive cranial diversification in frogs. *Nat. Commun.* **12**, 2503 (2021).
54. M. P. Neves *et al.*, Ecological shifts underlie parallels between ontogenetic and evolutionary allometries in parrotfishes. *Proc. R. Soc. B: Biol. Sci.* **291**, 20241897 (2024).
55. N. J. Gidmark, K. Pos, B. Matheson, E. Ponce, M. W. Westneat, "Functional morphology and biomechanics of feeding in fishes" in *Feeding in Vertebrates: Evolution, Morphology, Behavior, Biomechanics*, V. Bels, I. Q. Whishaw, Eds. (Springer, Cham, 2019), pp. 297–332.
56. D. R. Mitchell, E. Sherratt, V. Weisbecker, Facing the facts: Adaptive trade-offs along body size ranges determine mammalian craniofacial scaling. *Biol. Rev.* **99**, 496–524 (2024).
57. P. C. Wainwright, M. D. McGee, S. J. Longo, L. Patricia Hernandez, "Origins, innovations, and diversification of suction feeding in vertebrates" in *Integrative and Comparative Biology* (Oxford University Press, 2015), pp. 134–145.
58. R. Casaux, E. Barrera-Oro, Dietary overlap in inshore notothenioid fish from the Danco Coast, Western Antarctic Peninsula. *Polar Res.* **32**, 21319 (2013).
59. E. Moreira, M. Novillo, J. T. Eastman, E. Barrera-Oro, Degree of herbivory and intestinal morphology in nine notothenioid fishes from the western Antarctic Peninsula. *Polar Biol.* **43**, 535–544 (2020).
60. E. Moreira, M. Novillo, S. Gómez De Saravia, E. Barrera-Oro, Inter-annual dynamics in the trophic ecology of juveniles of five notothenioid fish species from the South Shetland Islands (Southern Ocean). *Polar Biol.* **46**, 993–1009 (2023).
61. G. P. Wagner, Homologues, natural kinds and the evolution of modularity. *Am. Zool.* **36**, 36–43 (1996).
62. J. Draghi, G. P. Wagner, Evolution of evolvability in a developmental model. *Evolution* **62**, 301–315 (2008).
63. J. T. Eastman, The nature of the diversity of Antarctic fishes. *Polar Biol.* **28**, 93–107 (2005).
64. C. I. Fraser, R. Nikula, D. E. Ruzzante, J. M. Waters, Poleward bound: Biological impacts of Southern Hemisphere glaciation. *Trends Ecol. Evol.* **27**, 462–471 (2012).

65. J. C. Svenning, W. L. Eiserhardt, S. Normand, A. Ordonez, B. Sandel, The influence of paleoclimate on present-day patterns in biodiversity and ecosystems. *Annu. Rev. Ecol. Evol. Syst.* **46**, 551–572 (2015).
66. E. M. Troyer *et al.*, The impact of paleoclimatic changes on body size evolution in marine fishes. *Proc. Natl. Acad. Sci. U.S.A.* **119**, e2122486119 (2022).
67. K. L. Ford *et al.*, A new era of morphological investigations: Reviewing methods for comparative anatomical studies. *Integr. Organism. Biol.* **5**, obad008 (2023).
68. A. L. Camp, T. J. Roberts, E. L. Brainerd, Swimming muscles power suction feeding in largemouth bass. *Proc. Natl. Acad. Sci. U.S.A.* **112**, 8690–8695 (2015).
69. D. Adams, M. Collyer, A. Kaliontzopoulou, E. Baken, Geomorph: Software for Geometric Morphometric Analyses (R package version 4.0.8, Comprehensive R Archive Network (CRAN), Vienna, Austria, 2024). https://CRAN.R-project.org/package=geomorph.
70. R Core Team, *R: A Language and Environment for Statistical Computing* (R Foundation for Statistical Computing, 2024).
71. D. Rhoda, P. D. Polly, C. Raxworthy, M. Segall, Morphological integration and modularity in the hyperkinetic feeding system of aquatic-foraging snakes. *Evolution* **75**, 56–72 (2021).
72. D. Rhoda, M. Segall, O. Larouche, K. Evans, K. D. Angielczyk, Local superimpositions facilitate morphometric analysis of complex articulating structures. *Integr. Comp. Biol.* **61**, 1892–1904 (2021).
73. B. Sidlauskas, Continuous and arrested morphological diversification in sister clades of characiform fishes: A phylomorphospace approach. *Evolution* **62**, 3135–3156 (2008).
74. E. Paradis, K. Schliep, ape 5.0: An environment for modern phylogenetics and evolutionary analyses in R. *Bioinformatics* **35**, 526–528 (2019).
75. D. C. Adams, A method for assessing phylogenetic least squares models for shape and other high-dimensional multivariate data. *Evolution* **68**, 2675–2688 (2014).
76. S. P. Blomberg, T. Garland, A. R. Ives, Testing for phylogenetic signal in comparative data: Behavioral traits are more labile. *Evolution* **57**, 717–745 (2003).
77. E. K. Baken, M. L. Collyer, A. Kaliontzopoulou, D. C. Adams, geomorph v4.0 and gmShiny: Enhanced analytics and a new graphical interface for a comprehensive morphometric experience. *Methods Ecol. Evol.* **12**, 2355–2363 (2021).
78. J. S. S. Denton, D. C. Adams, A new phylogenetic test for comparing multiple high-dimensional evolutionary rates suggests interplay of evolutionary rates and modularity in lanternfishes (Myctophiformes; Myctophidae). *Evolution* **69**, 2425–2440 (2015).
79. L. J. Harmon, J. A. Schulte II, A. Larson, J. B. Losos, Tempo and mode of evolutionary radiation in Iguanian lizards. *Science* **301**, 961–964 (2003).
80. G. J. Slater, M. W. Pennell, Robust regression and posterior predictive simulation increase power to detect early bursts of trait evolution. *Syst. Biol.* **63**, 293–308 (2014).
81. D. J. Murrell, A global envelope test to detect non-random bursts of trait evolution. *Methods Ecol. Evol.* **9**, 1739–1748 (2018).
82. S. Rutschmann *et al.*, Parallel ecological diversification in Antarctic notothenioid fishes as evidence for adaptive radiation. *Mol. Ecol.* **20**, 4707–4721 (2011).
83. E. C. Miller *et al.*, Alternating regimes of shallow and deep-sea diversification explain a species-richness paradox in marine fishes. *Proc. Natl. Acad. Sci. U.S.A.* **119**, e2123544119 (2022).
84. E. C. Miller, Comparing diversification rates in lakes, rivers, and the sea. *Evolution* **75**, 2055–2073 (2021).
85. I. G. Priede, *Deep-Sea Fishes: Biology, Diversity, Ecology and Fisheries* (Cambridge University Press, 2017).
86. S. T. Friedman, M. L. Collyer, S. A. Price, P. C. Wainwright, Divergent processes drive parallel evolution in marine and freshwater fishes. *Syst. Biol.* **71**, 1319–1330 (2022).
87. C. M. Martinez *et al.*, The deep sea is a hot spot of fish body shape evolution. *Ecol. Lett.* **24**, 1788–1799 (2021).
88. S. T. Friedman *et al.*, Body shape diversification along the benthic–pelagic axis in marine fishes. *Proc. R. Soc. B: Biol. Sci.* **287**, 20201053 (2020).
89. O. Larouche *et al.*, Reef-associated fishes have more maneuverable body shapes at a macroevolutionary scale. *Coral Reefs* **39**, 1427–1439 (2020).
90. K. M. Evans, K. L. Williams, M. W. Westneat, Do coral reefs promote morphological diversification? Exploration of habitat effects on labrid pharyngeal jaw evolution in the era of big data. *Integr. Comp. Biol.* **59**, 696–704 (2019).
91. K. M. Evans *et al.*, Beaks promote rapid morphological diversification along distinct evolutionary trajectories in labrid fishes (Eupercaria: Labridae). *Evolution* **77**, 2000–2014 (2023).
92. E. C. Miller *et al.*, Reduced evolutionary constraint accompanies ongoing radiation in deep-sea anglerfishes. *Nat. Ecol. Evol.* **9**, 474–490 (2024), 10.1038/s41559-024-02586-3.
93. R. Froese, D. Pauly, *FishBase 2000: Concepts, Design and Data Sources* (ICLARM, 2000).
94. A. Meade, M. Pagel, "BayesTraits V4.0.0." (University of Reading, United Kingdom, 2023). https://www.evolution.reading.ac.uk/BayesTraitsV4.0.0/BayesTraitsV4.0.0.html. Accessed 5 May 2024.
95. D. C. Adams, M. L. Collyer, Multivariate phylogenetic comparative methods: Evaluations, comparisons, and recommendations. *Syst. Biol.* **67**, 14–31 (2018).
96. A. Rambaut, A. J. Drummond, D. Xie, G. Baele, M. A. Suchard, Posterior summarization in Bayesian phylogenetics using Tracer 1.7. *Syst. Biol.* **67**, 901–904 (2018).
97. H. Ferguson-Gow, BTprocessR: A set of tools to help with the interpretation and analysis of the output of BayesTraits MCMC analyses. GitHub (2020). https://rdrr.io/github/hferg/BTprocessR/.
98. H. Ferguson-Gow, btrtools: A set of tools for processing and analysing the output of BayesTraits. GitHub (2017). https://rdrr.io/github/hferg/btrtools/.
99. G. S. Helfman, B. B. Collette, D. E. Facey, B. W. Bowen, Eds., *The Diversity of Fishes: Biology, Evolution, and Ecology* (Blackwell, ed. 2, 2009).
100. E. Kague *et al.*, Skeletogenic fate of zebrafish cranial and trunk neural crest. *PLoS One* **7**, e47394 (2012).
101. D. C. Adams, Evaluating modularity in morphometric data: Challenges with the RV coefficient and a new test measure. *Methods Ecol. Evol.* **7**, 565–572 (2016).
102. M. A. Conaway, D. C. Adams, An effect size for comparing the strength of morphological integration across studies. *Evolution* **76**, 2244–2259 (2022).
103. M. Pavlicev, J. M. Cheverud, G. P. Wagner, Measuring morphological integration using eigenvalue variance. *Evol. Biol.* **36**, 157–170 (2009).
104. D. C. Adams, R. N. Felice, Assessing trait covariation and morphological integration on phylogenies using evolutionary covariance matrices. *PLoS One* **9**, e94335 (2014).
105. M. P. Neves, H. W. Chan, E. C. Miller, K. M. Evans, Data from: Cranial modularity drives phenotypic diversification and adaptive radiation of Antarctic icefishes [Dataset]. Dryad. https://doi.org/10.5061/dryad.vq83bk44j. Deposited 5 September 2025.